

CONDUCTION AND INERTIA CORRECTION FOR TRANSIENT THERMOCOUPLE MEASUREMENTS. PART I: ANALYTICAL AND NUMERICAL MODELLING

Florian Seibold
Andreas Schwab
Victor Dubois

Rico Poser
Bernhard Weigand
Jens von Wolfersdorf

Institute of Aerospace Thermodynamics (ITLR), University of Stuttgart, D-70569, Stuttgart

ABSTRACT

Two-wire thermocouples are often used for temperature measurements. Under transient conditions, measurement errors can occur due to capacitive inertia and heat conduction along the stem of the thermocouples. The present study presents a correction of these thermocouple measurement errors caused by transient inertia and conductive effects using a simplified analytical approach and its numerical solution. Based on an energy balance the mathematical modelling is derived and analytically solved for specific boundary conditions. Further, numerical solutions have been implemented with different model complexities. Thereby the models show the significance of the necessary correction as well as the good agreement with theoretical considerations. A corresponding experimental validation is given in Part II.

NOMENCLATURE

A	m^2	area
Ar	-	aspect ratio
Bi	-	Biot number
c	$J\ kg^{-1}\ K^{-1}$	specific heat capacity
D	m	diameter
h	$W\ m^{-2}\ K^{-1}$	heat transfer coefficient
k	$W\ m^{-1}\ K^{-1}$	thermal conductivity
L	m	immersion length
m		index of eigenvalues
n		index of numerical time step
\vec{n}	-	normal vector
N		amount of control volumes
p		constant
Pr	-	Prandtl number
q	$W\ m^{-2}$	specific heat flux
Re	-	Reynolds number
t	s	time
T	K	temperature
u	$m\ s^{-1}$	velocity
\bar{u}	$m\ s^{-1}$	bulk velocity
V	m^3	volume
y	m	spatial coordinate
\tilde{y}	-	dimensionless coordinate

Greek symbols

α	$W\ m^{-2}\ K^{-1}$	contact coefficient
δ	-	time averaged error
Θ	-	dimensionless temperature
λ	-	eigenvalues
ν	$m^2\ s^{-1}$	kinematic viscosity
ρ	$kg\ m^{-3}$	density
τ	-	dimensionless time (Fourier number)

Subscripts

0	initial value
ana	analytical
c	cross-section
cond	heat conduction
conv	heat convection
corr	corrected
f	fluid
ideal	ideal
ref	reference
st	stationary
surf	thermocouple surface
TC	thermocouple
tr	transient
vol	volumetric
w	wall
∞	ambient

INTRODUCTION AND LITERATURE RESEARCH

The measurement of the thermodynamic state variable “temperature” is an essential prerequisite for many evaluation methods in thermodynamics. For example, heat exchange processes are mainly driven by temperature gradients at the wall and approximated by driving temperature differences between wall and fluid. Especially in transient processes, the precise measurement of these two temperature curves is a challenging task with different requirements in each case. While surface temperature measurements, e.g. by infrared thermography or thin-film sensors, practically represent a perfect thermal coupling of the measuring technique to the temperature to be

ANALYTICAL MODEL

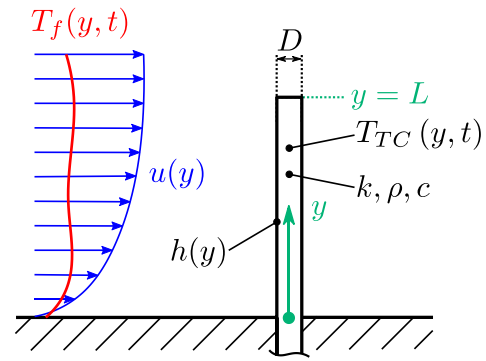


Fig. 2: Schematic setup of the investigated thermocouple

A schematic setup of a two-wire thermocouple in a cross flow situation is depicted in Fig. 2. At the probe surface a convective heat transfer occurs causing a specific heat flux $q_{conv} = h(y)(T_f(y, t) - T_{TC}(y, t))$. This convective mechanism reduces the difference between local fluid temperature $T_f(y, t)$ and local temperature in the thermocouple stem $T_{TC}(y, t)$. Consequently, a thermal coupling between the probe and its surrounding is created that enables precise measurements by recording the tip temperature $T_{TC}(y = L)$. However, real thermocouples feature tip temperatures $T_{TC}(y = L)$ that differ from the fluid temperature $T_f(y = L)$ due to two additional mechanisms. Firstly, in transient experiments the thermal inertia of the probe prevents the thermocouple to follow a change in fluid temperature immediately. Secondly, heat conduction $q_{cond} = -k\nabla T_{TC}$ in the thermocouple stem occurs. This second effect arises both in stationary as well as in transient experiments.

Modelling

In the following section an analytical equation is derived, which describes the previously mentioned mechanisms of thermal inertia and heat conduction. For this purpose, small Biot numbers $Bi_D = (hD)/k \ll 1$ are presumed, which ensure an immediate temperature equalization within a cross-section of the thermocouple. Consequently, a one-dimensional modelling approach is justified. Moreover, some assumptions are made in advance to further simplify the problem: First of all, the thermocouple consists of a cylinder with a constant diameter D that is made out of one single, homogeneous material with equivalent properties. Moreover, all material properties are constant and the flow velocity $u(y)$ is stationary. Finally, radiation is neglected.

measured, sensors in fluids are often difficult to integrate. In particular, the measured values of the widely used thermocouples can deviate significantly from the actual fluid temperature mainly due to two effects. First, due to thermal inertia, a thermocouple will always follow a transient temperature curve with a time delay. Second, due to temperature differences within the thermocouple, heat is conducted between the measuring tip and the rest of the thermocouple depending on its installation. The influence of both effects on the measurement data acquisition can be negligible or even lead to the measurement data being rendered completely useless. However, with the increasing necessity of measurements on small-scale, metallic original components, such as those resulting from additive manufacturing [1], both effects are increasingly no longer negligible as it is no longer possible to apply measures to sufficiently suppress the effects. Thus, methods are needed to compensate for the measured temperature at the thermocouple and predict the true fluid temperature as visualized in Fig. 1.

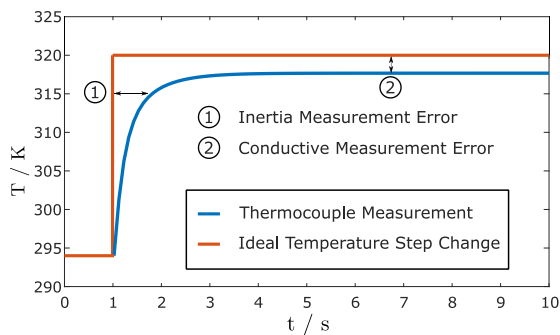


Fig. 1: Qualitative representation of inertia and conductive measurement errors

To compensate for thermal inertia, generic models using empiric time constants to be determined are common [2–13]. Differences due to unsteady heat conduction are, however, much more difficult to model, so that analytical, numerical, and empirical approaches can be found in the literature [14–21]. Especially models which can describe both effects simultaneously have hardly been developed and discussed in the past [22, 23]. This shortcoming is to be addressed by this work in two parts. In part I, a simplified analytical approach and its numerical solution will be presented. A model, based on an energy balance, is set up for specific boundary conditions and solved analytically. More complex cases are numerically predicted. The models confirm the significance of the necessary corrections and the good agreement with theoretical considerations. In part II [24], the models are applied and validated experimentally.

The latter equation (4) is a linear, partial differential equation of second order.

Closure of the Equation System

The differential equation (4) contains the unknown heat transfer coefficient h . This coefficient can be estimated by an appropriate Nusselt correlation for cylinders in cross-flow [25]

$$Nu(y) = C Re_D^m(y) Pr_f^n \left(\frac{Pr_f}{Pr_{f,surf}} \right)^p . \quad (5)$$

The index f represents fluid values, which are determined based on an average temperature of the fluid and thermocouple. In the course of this work, only the fluid temperature is used for this purpose in order to simplify the problem. Furthermore, $Pr_{f,surf}$ represents the Prandtl number of the fluid based on the temperature at the thermocouple surface. Moreover, the constants C , m and n are given in [25].

The local Reynolds number $Re_D = (u(y) D)/\nu$ in Eq. (5) depends on the local flow velocity $u(y)$ at the thermocouple stem. In general, any velocity distribution can be used for estimating the local Reynolds number. Under real measurement conditions, however, the exact distribution might be unknown. Therefore, a uniform velocity profile $u(y) = \bar{u}$ with its bulk velocity \bar{u} is assumed in order to keep the model simple.

When further taking into account the definition of the Nusselt number $Nu = (hD)/\lambda_f$, the equation for the heat transfer coefficient h yields

$$h = C \frac{\lambda_f}{D} \left(\frac{\bar{u}D}{\nu} \right)^m Pr_f^n \left(\frac{Pr_f}{Pr_{f,surf}} \right)^p . \quad (6)$$

This equation for h is only valid for thermocouples with circular cross-section, which are installed in cross-flow situations. In general, the model is also applicable for non-circular cross-sections and non-cross-flow situations if appropriate Nusselt correlations are available.

Boundary conditions are necessary to close the equation system including the fluid temperature $T_f(y, t)$, the initial temperature of the thermocouple $T_{TC}(y, t = 0)$ as well as boundary conditions for the thermocouple tip $T_{TC}(y = L, t)$ and at the wall $T_{TC}(y = 0, t)$. These boundary conditions depend on the experimental setup and, thus, are case specific.

Non-Dimensional Model

In case of simple boundary conditions Eq. (4) can be solved analytically. For this purpose, an isothermal initial temperature $T_0(y) = \text{const.}$ is assumed and an ideal jump in fluid temperature is enforced at $t = 0$. The thermocouple tip is modelled with an adiabatic boundary condition

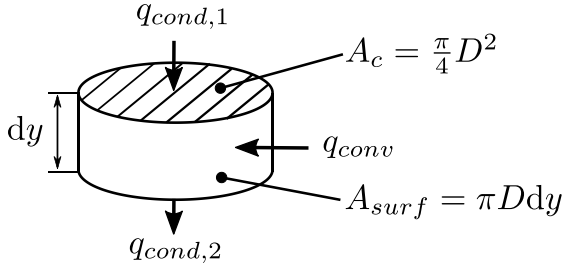


Fig. 3: Infinitesimal segment of the thermocouple

The energy balance for an infinitesimal segment of the thermocouple can be derived from Fig. 3 yielding

$$\begin{aligned} & \underbrace{\int_V \rho c \frac{\partial T_{TC}(y, t)}{\partial t} dV}_{\text{thermal inertia}} \\ &= \underbrace{\int_{A_c} k \nabla T_{TC}(y, t) \cdot \vec{n} dA_c}_{\text{conduction}} \\ &+ \underbrace{\int_{A_{surf}} h(y) (T_F(y) - T_{TC}(y, t)) dA_{surf}}_{\text{convection}} . \end{aligned} \quad (1)$$

Here, the variables c , ρ and k represent heat capacity, density and heat conductivity, respectively. These properties are considered to be constant. Due to the small Biot number Bi , the convective heat transfer in Eq. (1) can be modelled as volumetric heat source

$$\begin{aligned} q_{vol} &= q_{conv} \frac{dA_{surf}}{dV} \\ &= \frac{4}{D} h(y) (T_F(y) - T(y, t)) . \end{aligned} \quad (2)$$

Further, the surface integral of the heat conduction term in Eq. (1) is replaced by a volumetric integral using the Gauss theorem. The energy balance then results in

$$\begin{aligned} & \int_V \left[\rho c \frac{\partial T_{TC}(y, t)}{\partial t} - \nabla \cdot (k \nabla T_{TC}(y, t)) \right. \\ & \left. - \frac{4}{D} h(y) (T_F(y) - T_{TC}(y, t)) \right] dV = 0 . \end{aligned} \quad (3)$$

Here, $a = k/(\rho c)$ represents the thermal diffusivity. Equation (3) must be satisfied for an arbitrary control volume, which is only possible in case of a vanishing integrand

$$\begin{aligned} & \frac{\partial T_{TC}(y, t)}{\partial t} - a \frac{\partial^2 T_{TC}(y, t)}{\partial y^2} \\ & - \frac{4}{\rho c D} h(y) (T_F(y) - T_{TC}(y, t)) = 0 . \end{aligned} \quad (4)$$

$\partial T_{TC}/\partial y|_{y=L} = 0$ and the temperature at the wall is assumed to be isothermal with $T_{TC}(y=0) = T_W = T_0$. Moreover, a constant heat transfer coefficient h is considered that corresponds to a uniform velocity profile.

Before solving Eq. (4), it can be transformed into a non-dimensional formulation using the following dimensionless variables:

- temperature $\Theta = \frac{T_{TC}-T_f}{T_0-T_f}$
- time (Fourier number) $\tau = \frac{at}{L^2}$
- coordinate $\tilde{y} = \frac{y}{L}$
- aspect ratio $Ar = \frac{L}{D}$
- Biot number $Bi_L = \frac{hL}{k}$

The non-dimensional equation then yields

$$\frac{\partial \Theta(\tilde{y}, \tau)}{\partial \tau} - \frac{\partial^2 \Theta(\tilde{y}, \tau)}{\partial \tilde{y}^2} + 4Bi_L Ar \Theta(\tilde{y}, \tau) = 0 \quad (7)$$

in case of constant material properties. The corresponding boundary conditions are

$$\Theta(\tilde{y}, \tau = 0) = 1, \quad (8)$$

$$\Theta(\tilde{y} = 0, \tau) = 1 \quad \text{and} \quad (9)$$

$$\left. \frac{\partial \Theta(\tilde{y}, \tau)}{\partial \tilde{y}} \right|_{\tilde{y}=1} = 0. \quad (10)$$

The definition of the dimensionless temperature Θ achieves a homogeneous differential equation, while the boundary conditions given by Eqs. (8) and (9) become inhomogeneous. To address this problem, the solution will be split up into a stationary part $\Theta_{st}(\tilde{y})$, which satisfies the inhomogeneous boundary condition of Eq. (9), and a transient part $\Theta_{tr}(\tilde{y}, \tau)$. Due to the linear character of Eq. (7), the solution can be superimposed from the stationary and the transient part of the solution as

$$\Theta(\tilde{y}, \tau) = \Theta_{st}(\tilde{y}) + \Theta_{tr}(\tilde{y}, \tau). \quad (11)$$

The stationary solution $\Theta_{st}(\tilde{y})$ is not a function of time. Consequently, the partial differential Eq. (7) reduces to an ordinary one

$$-\frac{d^2 \Theta_{st}(\tilde{y})}{d\tilde{y}^2} + 4Bi_L Ar \Theta(\tilde{y}) = 0 \quad (12)$$

with the general solution

$$\Theta_{st}(\tilde{y}) = c_1 \sinh(p\tilde{y}) + c_2 \cosh(p\tilde{y}). \quad (13)$$

Here, $p = 2\sqrt{Bi_L Ar}$ represents a constant. When further taking into account the boundary conditions from Eqs. (9) and (10), the stationary solution yields

$$\Theta_{st}(\tilde{y}) = -\tanh(p) \sinh(p\tilde{y}) + \cosh(p\tilde{y}). \quad (14)$$

The transient solution $\Theta_{tr}(\tilde{y}, \tau)$ is predicted by introducing the separation approach $\Theta_{tr}(\tilde{y}, \tau) = G(\tilde{y})H(\tau)$ into Eq. (7):

$$\frac{1}{H(\tau)} \frac{\partial H(\tau)}{\partial \tau} + 4Bi_L Ar = \frac{1}{G(\tilde{y})} \frac{\partial^2 G(\tilde{y})}{\partial \tilde{y}^2} = -p^2. \quad (15)$$

The right and left hand side in Eq. (15) depend on a single but different variable and, thus, must equal a constant value. As a result, the partial differential equation is subdivided into two ordinary differential equations with the corresponding boundary conditions

$$G(\tilde{y})H(\tau = 0) = 1 - \Theta_{st}(\tilde{y}), \quad (16)$$

$$G(\tilde{y} = 0) = 0 \quad \text{and} \quad (17)$$

$$\left. \frac{\partial G}{\partial \tilde{y}} \right|_{\tilde{y}=1} = 0. \quad (18)$$

The general solution for $G(\tilde{y})$ is

$$G(\tilde{y}) = c_3 \sin(\lambda_{tr}\tilde{y}) + c_4 \cos(\lambda_{tr}\tilde{y}). \quad (19)$$

When further considering the boundary conditions from Eq. (17) and (18), the specific solution yields

$$G_m(\tilde{y}) = c_{4,m} \cos(\lambda_{tr,m}\tilde{y}). \quad (20)$$

Here, $\lambda_{tr,m} = (2m-1)\pi/2$ contains an infinite amount of eigenvalues with $m = 1, 2, 3, \dots$

Moreover, the general solution for $H_m(\tau)$ is

$$H_m(\tau) = c_{5,m} e^{-(p^2 + \lambda_{tr,m}^2)\tau}. \quad (21)$$

Since these results for $G_m(\tilde{y})$ and $H_m(\tau)$ are not able to satisfy the condition for the initial temperature in Eq. (16), the result is expanded into an infinite series in order to consider not only one but all eigenvalues $\lambda_{tr,m}$:

$$\Theta_{tr}(\tilde{y}, \tau) = \sum_{m=1}^{\infty} G_m(\tilde{y})H_m(\tau). \quad (22)$$

Then, the solution for the dimensionless temperature reads

$$\begin{aligned}\Theta(\tilde{y}, \tau) &= \Theta_{st}(\tilde{y}) + \Theta_{tr}(\tilde{y}, \tau) \\ &= -\tanh(p) \sinh(p\tilde{y}) + \cosh(p\tilde{y}) \\ &\quad + \sum_{m=1}^{\infty} a_m \sin(\lambda_{tr,m} \tilde{y}) e^{-(p^2 + \lambda_{tr,m}^2)\tau}.\end{aligned}\quad (23)$$

Finally, the remaining constant $a_m = c_{4,m}c_{5,m}$ can be derived from the initial condition in Eqs. (8) and (16) to

$$a_m = \frac{2p^2}{\lambda_{tr,m}(\lambda_{tr,m}^2 + p^2)}.\quad (24)$$

DISCUSSION OF THE ANALYTICAL RESULTS

The analytical solution given by Eq. (23) allows a deeper insight into the thermal processes of thermocouples. Therefore, the characteristic behavior of the results will be analyzed in the following section.

For the considered boundary conditions, the solution depends on two main parameters. These are the constant $p = 2\sqrt{\text{Bi}_L \text{Ar}}$, which contains the impact of heat conduction and convection, and the Fourier number $\tau = (at)/L^2$ representing the influence of time. In Fig. 4, an exemplary solution for the thermocouple tip temperature $\Theta(\tilde{y} = 1, \tau)$ is depicted over time for a value of $p = 2\sqrt{2}$. These dimensionless values $\Theta(\tilde{y} = 1, \tau)$ illustrate the relative difference between measured temperatures and real fluid temperatures in experiments. Moreover, an ideal thermocouple is shown for comparison, which records the real fluid temperature.

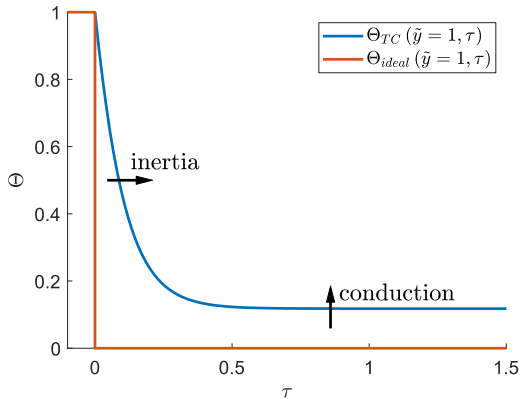


Fig. 4: Analytical solution of the thermocouple tip temperature for $p = 2\sqrt{\text{Bi}_L \text{Ar}} = 2\sqrt{2}$

In Fig. 4 two major effects can be observed that are inertia and conductive stem effect. Firstly, the thermal inertia is caused by the transient part of the solution $\Theta_{tr}(\tilde{y}, \tau)$, which delays the thermocouple's reaction when a change in fluid temperature is imposed. Consequently, a significant

deviation between tip temperature and real fluid temperature arises for small Fourier numbers τ leading to high values of $\Theta(\tilde{y} = 1, \tau)$. For large Fourier numbers τ , however, the inertia impact vanishes due to the exponential function in Eq. (23):

$$\lim_{\tau \rightarrow \infty} \Theta_{tr}(\tilde{y} = 1, \tau) = 0.\quad (25)$$

Secondly, the conductive stem effect can be observed in Fig. 4. This effect considers heat conduction and convection at the thermocouple stem leading to a deviation between the thermocouple tip temperature and the fluid temperature. The conductive stem effect is incorporated in the analytical solution in Eq. (23) via the constant $p = 2\sqrt{\text{Bi}_L \text{Ar}}$. Consequently, this process not only affects the stationary part of the solution $\Theta_{st}(\tilde{y})$ but also the transient one $\Theta_{tr}(\tilde{y}, \tau)$. As a result, the conductive stem effect does not vanish for large Fourier numbers τ :

$$\lim_{\tau \rightarrow \infty} \Theta(\tilde{y} = 1, \tau) = \Theta_{st}(\tilde{y} = 1).\quad (26)$$

To conclude, the relative importance of inertia and conduction depend on the dimensionless parameters p and τ . For small values of τ inertia dominates whereas the conductive stem effect prevails for large values of τ .

In the introduction section, different modelling approaches for the inertia effect were introduced from literature. The most popular approach depends on an exponential function containing a single time constant, which describes the transient behavior of the thermocouple tip temperature. However, when additionally taking into account the conductive stem effect this modelling approach fails. The conduction effect, which is incorporated in $p = 2\sqrt{\text{Bi}_L \text{Ar}}$, affects not only the stationary part of the solution $\Theta_{st}(\tilde{y})$ but also the transient one $\Theta_{tr}(\tilde{y}, \tau)$. Consequently, the time dependency of $H_m(\tau)$ in Eq. (21) requires an infinite amount of time constants $\lambda_{tr,m}^2$ instead of a single constant. Therefore, a single time constant is not able to resolve the combined impact of inertia and conductive stem effect in thermocouples. Instead, the partial differential Eq. (7) must be solved. However, analytical solutions exist only for simple boundary conditions, which are not able to describe real measurement situations. Therefore, a numerical model is required that allows a wider range of boundary conditions.

NUMERICAL MODEL

To overcome the restrictions of the analytical solution, a numerical model was developed. For this purpose, a finite volume approach is derived that allows more suitable boundary conditions in

order to increase the model accuracy. Thus, arbitrary velocity distributions $u(y)$, time dependent fluid temperatures $T_f(t)$ and more complex boundary conditions for the thermocouple stem at the wall are considered. Apart from that, the condition at the tip remains unchanged still using the assumption of an adiabatic surface.

The boundary condition at the wall is modified by extending the thermocouple stem into the wall according to Fig. 5. Here, the conductive heat transfer between wall and thermocouple is modelled using a contact coefficient α_w , which is assumed to be constant over time. Moreover, outside of the wall an adiabatic condition is prescribed.

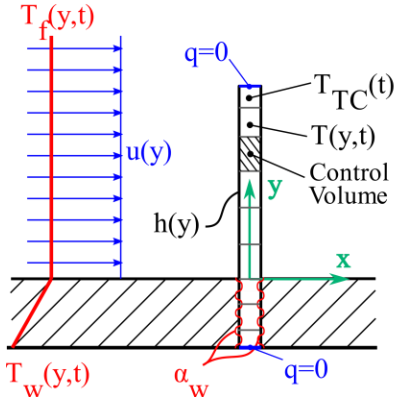


Fig. 5: Computational domain and boundary conditions

The finite volume approach can be deduced based on the integral form in Eq. (1). For this purpose, the domain is divided into N control volumes as shown in Fig. 5. Within each of these volumes the field variables exhibit constant values. Equation (1) is discretized using an implicit scheme in time of first order and a central difference scheme of second order for all spatial heat fluxes [26]. Then, the governing equation for each control volume i yields

$$\begin{aligned} & \rho c \frac{T_i^{n+1} - T_i^n}{\Delta t} A_c \Delta y \\ &= k \frac{T_{i-1}^{n+1} - 2T_i^{n+1} + T_{i+1}^{n+1}}{\Delta y} A_c \\ & \quad + h_i^{n+1} (T_{ref,i}^{n+1} - T_i^{n+1}) A_{surf} . \end{aligned} \quad (27)$$

Depending on the y -coordinate within the stem, the heat transfer coefficient between the thermocouple and its surrounding changes. It can be either a convective exchange within the fluid at $y_i \geq 0$ or a conductive exchange inside the wall at $y_i < 0$. Equation (26) combines both effects in a single equation by defining the variables h_i and $T_{ref,i}^n$ in as follows:

$$\begin{aligned} h_i &= \begin{cases} h_{f,i} & \forall y_i \geq 0 \\ \alpha_w & \forall y_i < 0 \end{cases} \\ T_{ref,i}^n &= \begin{cases} T_{f,i}^n & \forall y_i \geq 0 \\ T_{w,i}^n & \forall y_i < 0 \end{cases} . \end{aligned} \quad (28)$$

Here, $T_{w,i}^n$ denotes the local wall temperature that can be approximated by an arbitrary temperature distribution between the fluid temperature T_f and the ambient temperature T_∞ . The model is implemented in MATLAB.

Unfortunately, in the numerical model in Eqs. (26) and (27) several model parameters exist that are unknown for real thermocouples. These are the density ρ , heat capacity c , conductivity k and contact coefficient α_w . This issue of the unknown parameters will be addressed at the end of the paper.

Validation

Disregarding the unknown parameters, the numerical model can be validated by comparing its outcomes to the analytical solution given by Eq. (23). For this purpose, the thermocouple stem within the wall is omitted and the model parameters are defined such that they satisfy the non-dimensional parameter $p = 2\sqrt{Bi_L Ar} = 2\sqrt{2}$. A uniform velocity profile is prescribed that causes a uniform heat transfer coefficient h and, thus, a uniform Biot-number Bi_L along the thermocouple stem. Furthermore, all boundary and initial conditions are defined in accordance with Eqs. (15) - (17) implying an isothermal initial temperature $T_{TC}(y, t = 0)$ and an ideal jump in fluid temperature T_f . As a result, the implementation of the numerical model as well as its grid dependency can be validated.

For comparison of analytical and numerical results a transformation is necessary since the analytical outcomes contain non-dimensional values whereas the numerical model predicts absolute values. Therefore, the numerical results are converted into non-dimensional temperatures Θ_{num} . The validation is then conducted by averaging the error δ between analytical and numerical temperatures at the thermocouple tip over a time period of $t = 5$ s ($\tau = 64 \cdot 10^4$):

$$\delta = \frac{1}{N} \sum_{n=1}^N |\Theta_{ana}(\tilde{y} = 1, \tau^n) - \Theta_{num}(\tilde{y} = 1, \tau^n)| . \quad (29)$$

The error δ for different resolutions in time and space is illustrated in Fig. 6. The temporal resolution is depicted in absolute values Δt_i since these values were prescribed for the numerical

model. The corresponding non-dimensional time steps $\Delta\tau_i$ are given in Tab. 1.

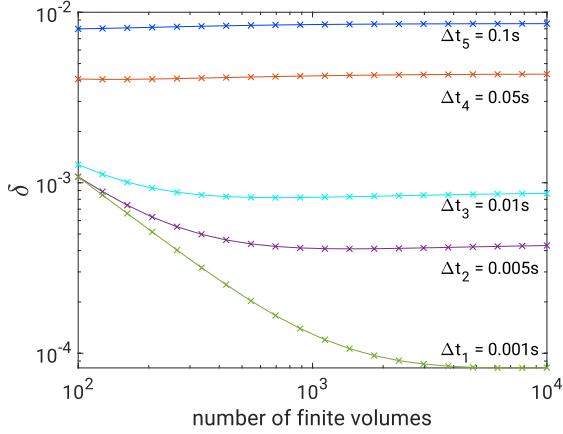


Fig. 6: Summarized error for different resolutions in time and space for $p = 2\sqrt{Bi_L Ar} = 2\sqrt{2}$

Tab. 1: Absolute time steps Δt_i and its corresponding non-dimensional values $\Delta\tau_i$

	$i = 1$	$i = 2$	$i = 3$	$i = 4$	$i = 5$
Δt_i [s]	0.001	0.005	0.01	0.05	0.1
$\Delta\tau_i$ [10^2]	1.24	6.2	12.4	62	124

In general, the error in Fig. 6 shows small deviations between analytical and numerical results. The model is, thus, implemented properly. Furthermore, a resolution of 500 control volumes in combination with a time step of $\Delta t = 0.01$ s is sufficient to reach accurate results with an error of $\delta < 10^{-3}$. Hence, this resolution is used for subsequent numerical investigations.

Fluid Temperature Correction

In experiments, one intends to measure the real fluid temperature. However, thermocouples only measure its tip temperature $T_{TC}(y = L)$, which deviates from the real fluid temperature T_f . Therefore, the subsequent section uses the above introduced numerical model in order to recompute the real fluid temperatures from the thermocouple tip temperatures. In the following, such an inverse calculation is also termed fluid temperature correction.

Based on the discretized Eq. (26) a correction calculation is possible, if two requirements are satisfied: Firstly, the time dependent measurement data $T_{TC}(y = L, t)$ is required from experimental investigation. This measurement needs to start from thermal equilibrium. Secondly, the initial temperature of the thermocouple $T_{TC}(y, t = 0)$ and the model parameters need to be known. As a result, the unknown values in Eqs. (26) and (27) are the fluid temperatures of the actual and the preceding time steps T_f^{n+1} and T_f^n as well as the thermocouple temperatures $T_{TC}^n(y < L, t)$. Within the thermocouple only the tip temperature $T_{TC}^n(y = L, t)$ is known from the experiments. The

unknown temperatures can then be computed successively beginning at the first time step by taking into account the initial condition, which is the thermal equilibrium.

The capability of such an inverse calculation can be demonstrated on the basis of the analytical solution from Eq. (23). For this purpose, the thermocouple stem within the wall is omitted as already mentioned for the validation. Moreover, the boundary and initial conditions are again defined such that they satisfy the non-dimensional parameter $p = 2\sqrt{Bi_L Ar} = 2\sqrt{2}$.

The analytical solution from Eq. (23) for the thermocouple tip temperature $\Theta_{TC}(\tilde{y} = 1, \tau)$ as well as the results for an ideal probe $\Theta_{ideal}(\tilde{y} = 1, \tau)$ are depicted in Fig. 7. The latter represents a perfect probe that is neither affected by inertia nor by the conductive stem effect. Additionally, the numerical results from the fluid temperature correction are illustrated in Fig. 7 as non-dimensional values $\Theta_{f,corr}(\tau)$. These were recomputed from the analytical solution $\Theta_{TC}(\tilde{y} = 1, \tau)$.

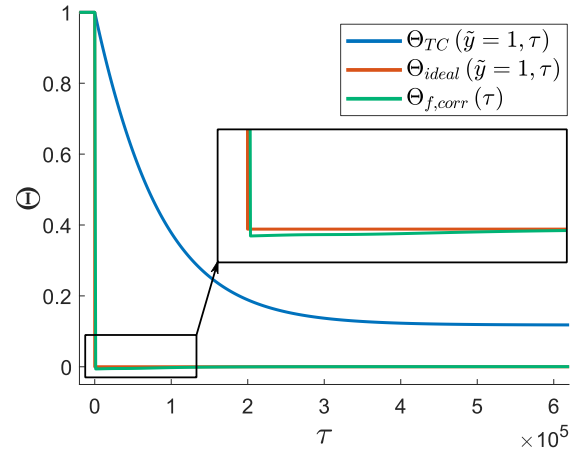


Fig. 7: Fluid temperature correction for $p = 2\sqrt{Bi_L Ar} = 2\sqrt{2}$ using 500 control volumes and a time step of $\Delta\tau = 1240$

When comparing the recomputed fluid temperatures $\Theta_{f,corr}(\tau)$ and the ideal probe $\Theta_{ideal}(\tilde{y} = 1, \tau)$, the curves show a perfect match. Immediately after the temperature jump a maximum deviation of $|\Theta_{f,corr}(\tau) - \Theta_{ideal}(\tilde{y} = 1, \tau)| \approx 6.2 \cdot 10^{-3}$ occurs.

As a result, an inverse calculation of the fluid temperature based on measurement data is possible if the model parameters are known. This procedure represents a correction calculation that eliminates the combined impact of inertia and conductive stem effect in thermocouple measurements.

Determination of model parameters

The preceding section proved the capability of the fluid temperature correction. However, a major problem remains that is the determination of the

unknown model parameters. For real thermocouples the material density ρ , heat conductivity k , heat capacity c and the contact coefficient α_w are unknown. Without knowledge of these parameters the equation system remains under-determined.

To resolve this problem, the following procedure is proposed: According to Fig. 8, two identical thermocouples are mounted in a flow channel such that they are exposed to a cross flow situation. The immersion length of these probes differ but their tips are close together without touching each other. Due to their spatial vicinity, both tips are exposed to the same fluid temperature T_f . However, the thermocouple tip temperatures $T_{Tc}(y=L)$ differ because of the different immersion lengths that impact the conductive stem effect.

For the determination of the model parameters a single experiment is required, which is also termed calibration measurement in the following. This calibration measurement starts from thermal equilibrium and imposes a strong change in fluid temperature while recording both thermocouples simultaneously with a high sampling rate. Attention needs to be paid that no time offset between the measured data of the different thermocouples occurs. Moreover, high measurement accuracy is essential.

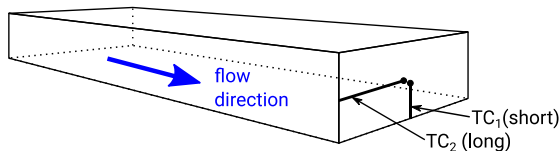


Fig. 8: Experimental setup for determination of the model parameters

The numerical model of the calibration experiment combines both thermocouples and, thus, involves five unknown parameters: $k_1 = k_2$, $c_1 = c_2$, $\rho_1 = \rho_2$, α_{w1} and α_{w2} . In order to determine these parameters an initial guess is required. Based on this initial guess the model is able to recompute the fluid temperature for each of the two thermocouples. Most likely, these recomputed fluid temperatures do not coincide and hence the model parameters need to be modified. Therefore, the calibration calculation optimizes the parameters until the recomputed fluid temperatures coincide for every measured time step. The calibration calculation then yields a best fit match for the unknown model parameters.

Finally, some considerations on the parameter determination are drawn in order to improve the physical understanding of the model: The numerical model incorporates several assumptions and simplifications that are not in accordance with the conditions in real experimental investigations. Therefore, the model contains some inaccuracies.

By conducting the parameter calculation, the numerical algorithm aims to compensate these inaccuracies as best as possible in order to satisfy the condition of the same fluid temperature T_f for both thermocouples. Hence, the resulting parameters can be understood as calibrated model coefficients, which do not necessarily reflect the real material properties and the real contact coefficients. This, furthermore, implies that the model parameters strongly depend on the prescribed boundary conditions such as wall temperature distribution and velocity profile.

The preceding section demonstrated that all unknown model parameters can be determined and the model, thus, works from a theoretical point of view. Part II of this paper [1] continues at this point by addressing the practical application of the model for real experimental investigations.

CONCLUSION

Considering two-wire thermocouples two major measurement errors were investigated: a capacitive inertia effect and a conductive stem effect. In this context an analytical model was set up including the transient behaviour of a thermocouple's heat conducting stem.

In case of simple boundary conditions like an adiabatic thermocouple tip, an isothermal wall and an ideal jump in fluid temperature, the corresponding analytical solution was derived. While the inertia effect is predominant in small timescales the conductive stem effect occurs at larger timescales. Even though time delaying transient inertia effects are commonly corrected in literature by a time constant correction of an exponential function it was shown that this procedure is not applicable when considering the combined impact of inertia and conductive stem effect in thermocouples. Due to the shape of the solution of a linear superposition of stationary and transient solutions, an infinite amount of superimposed time constants respectively eigenvalues of the solution are necessary.

Because of even more complex boundary conditions in measurement applications a by far more flexible numerical model was developed. A validation and grid study based upon the analytical solution was performed. Moreover, an inverse calculation method is introduced recalculating the real fluid temperature out of measurement data. In a comparison with the analytical solution for an ideal temperature jump the numerical recalculation verifiably shows the elimination of the combined inertia and conduction effect. Nevertheless, the material properties represented as numerical model coefficients remain unknown until an experimental calibration is executed. Such one is shown in rough outlines and its application will further be demonstrated in Part II [24].

To sum up, the theoretical considerations are represented by an analytical solution and further met fully by the introduced numerical simulations, but still require experimental validation data. It is envisioned, that by an identification of various thermocouple types and reproducible installation a correction of the measurement errors can be generalized.

ACKNOWLEDGMENTS

The authors would acknowledge the funding of this project by the German Research Foundation (DFG) under the Grant No. WE 2549/38-1 and in the framework of the Collaborative Research Centre Transregio 40.

REFERENCES

[1] S. Naik, S. Retzko, M. Gritsch, and A. Sedlov, "Impact of Turbulator Design on the Heat Transfer in a High Aspect Ratio Passage of a Turbine Blade," in *ASME Turbo Expo 2014: Turbine Technical Conference and Exposition*, Düsseldorf, Germany, Jun. 2014.

[2] M. Jaremkiewicz, "Accurate Measurement of Unsteady State Fluid Temperature," *Heat Mass Transfer*, vol. 53, no. 3, pp. 887–897, 2016.

[3] K. Konopka, "Thermocouple Dynamic Errors Correction for Instantaneous Temperature Measurements in Induction Heating," in *19th IMEKO TC 4 Symposium and 17th IWADC Workshop*.

[4] A. Terzis, J. von Wolfersdorf, B. Weigand, and P. Ott, "Thermocouple Thermal Inertia Effects on Impingement Heat Transfer Experiments using the Transient Liquid Crystal Technique," *Measurement Science and Technology*, vol. 23, no. 11, 2012.

[5] M. Tagawa, K. Kaifuku, T. Houra, Y. Yamagami, and K. Kato, "Response Compensation of fine-wire Thermocouples and its Application to Multidimensional Measurement of a Fluctuating Temperature Field," *Heat Trans. Asian Res.*, vol. 40, no. 5, pp. 404–418, 2011.

[6] S. Nikonov and K. Velkov, "Accounting for the Inertia of the Thermocouples' Measurements by Modelling of a NPP Kalinin-3 Transient with the Coupled System Code ATHLET-BIPR-VVER," in *Proceedings of the eighteenth symposium of atomic energy research*.

[7] K. Farahmand and J. W. Kaufman, "Experimental Measurement of fine Thermocouple Response Time in Air," *Experimental Heat Transfer*, vol. 14, no. 2, pp. 107–118, 2001.

[8] S. J. Park and S. T. Ro, "A new Method for measuring Time Constants of a Thermocouple Wire in Varying Flow States,"

The 17th Symposium on Measuring Techniques in Transonic and Supersonic Flow in Cascades and Turbomachines

Experiments in Fluids, vol. 21, no. 5, pp. 380–386, 1996.

[9] P. C. Miles and F. C. Gouldin, "Determination of the Time Constant of Fine-Wire Thermocouples for Compensated Temperature Measurements in Premixed Turbulent Flames," *Combustion Science and Technology*, vol. 89, 1-4, pp. 181–199, 1993.

[10] C. Petit, P. Gajan, J. C. Lecordier, and P. Paranthoen, "Frequency Response of fine wire Thermocouple," *J. Phys. E: Sci. Instrum.*, vol. 15, no. 7, pp. 760–770, 1982.

[11] A. Ballantyne and J. B. Moss, "Fine Wire Thermocouple Measurements of Fluctuating Temperature," *Combustion Science and Technology*, vol. 17, 1-2, pp. 63–72, 1977.

[12] G. M. Levin and V. I. Vol'mir, "Methods for Testing Thermal Inertia in Thermocouples and Resistance Thermometers," *Meas Tech*, vol. 3, no. 4, pp. 309–313, 1960.

[13] M. D. Scadron and I. Warshasky, "Experimental Determination of Time Constants and Nusselt Numbers for Bare-Wire Thermocouples in High-Velocity Air Streams and Analytic Approximation of Conduction and Radiation Errors," *Technical Report NACA-TN-2599*, 1952.

[14] Z. Zou, Weiping Yang, Weihao Zhang, Xiaokui Wang, and Jian Zhao, "Numerical Modeling of Steady State Errors for Shielded Thermocouples based on Conjugate Heat Transfer Analysis," *International Journal of Heat and Mass Transfer*, vol. 119, pp. 624–639, 2018.

[15] M. Axtmann, J. von Wolfersdorf, and G. Meyer, "Application of the Transient Heat Transfer Measurement Technique in a Low Aspect Ratio Pin Fin Cooling Channel," in *ASME Turbo Expo 2015: Turbine Technical Conference and Exposition*, Montreal, Quebec, Canada, Jun. 2015.

[16] Chris J. Kobus, "True Fluid Temperature Reconstruction Compensating for Conduction Error in the Temperature Measurement of Steady Fluid Flows," *Review of Scientific Instruments*, vol. 77, no. 3, 2006.

[17] R. J. Dickinson, "Thermal Conduction Errors of Manganin-Constantan Thermocouple Arrays," *Phys. Med. Biol.*, vol. 30, no. 5, pp. 445–453, 1985.

[18] B. S. Singh and A. Dybbs, "Error in Temperature Measurements due to Conduction along the Sensor Leads," *Journal of Heat Transfer*, vol. 98, no. 3, pp. 491–495, 1976.

[19] G. J. K. Packer and J. L. B. Gamlen, "Calculation of Temperature Measurement Errors in Thermocouples in Convection Heating Cans," *J Food Science*, vol. 39, no. 4, pp. 739–743, 1974.

- [20] W. G. Hess, "Thermocouple Conduction Error with Radiation Heat Loss," Master thesis, Department of Aerospace and Mechanical Engineering, University of Arizona, 1965.
- [21] L. M. K. Boelter and R. W. Lockhart, *Thermocouple Conduction Error observed in Measuring Surface Temperatures*: National Advisory Committee for Aeronautics, 1951.
- [22] S. M. Khine, T. Houra, and M. Tagawa, "Heat-Conduction Error of Temperature Sensors in a Fluid Flow with Nonuniform and Unsteady Temperature Distribution," *The Review of scientific instruments*, vol. 84, no. 4, 2013.
- [23] Chris J. Kobus, "True-Temperature Reconstruction from Combined Conduction and Transient Thermocouple Temperature Lag Errors in Single-Phase Convection," in *ASME 2013 Heat Transfer Summer Conference*, 10.1115/HT2013-17094.
- [24] T. Krille, M. Diehl, R. Poser, and J. von Wolfersdorf, "Conduction and Inertia Correction for Transient Thermocouple Measurements. Part II: Experimental Validation and Application," in *The 17th Symposium on Measuring Techniques in Transonic and Supersonic Flow in Cascades and Turbomachines*.
- [25] H. D. Baehr and K. Stephan, *Wärme- und Stoffübertragung*, 9th ed.: Springer-Verlag Berlin Heidelberg, 2016.
- [26] C.-D. Munz and T. Westermann, *Numerische Behandlung gewöhnlicher und partieller Differenzialgleichungen: Ein interaktives Lehrbuch für Ingenieure*, 3rd ed. Berlin: Springer Vieweg, 2012.